Polarization in Light-scattering by Aerosol

Akiyoshi MATSUZAKI
The Institute of Space and Astronautical Science, Komaba 4-6-1, Meguro-ku, Tokyo 153
(Received April 5, 1985)

The polarization of the light scattered by aerosol has been studied by the theoretical calculation based on the Mie scattering theory. The present calculation obtains the polarization of the light scattered by aerosol as a function of size parameter, *i.e.* $x=2\pi r/\lambda$, where r and λ are the radius of aerosol and the wavelength of the scattered light, respectively, for various refractive indexes. These results give the useful informations for the experimental study on the size-growth in aerosol formation by the measurement of the scattered light polarization. The characteristic of the scattered light intensity, which is usually used as a kind of concentration parameter in the study on aerosol formation, is also discussed.

The investigation on aerosols, which are small particles floating in the atmosphere, is of great importance in view of chemical reaction and environmental science. For example, aerosol formation includes heterogeneous reactions, *i.e.*, gaseous molecules and solid, gas and liquid, or liquid and solid. On the other hand, in view of environmental science, the stratospheric aerosol is known to affect the radiation balance in the atmosphere. Consequently, it is very important with the relevance to the climate problem. Its property and formation mechanism are the up-to-date targets.

In the study on aerosol, the scattered light intensity is usually used as a kind of concentration parameter. Namely, the property of aerosol, *e.g.* the size, the refractive index, *etc.*, has been studied by the measurement of the polarization and the angular distribution of the scattered light. However, in fact, these show the complex dependence on the size and the refractive index of aerosol and the wavelength of the scattered light. In this situation, the present work made the theoretical calculation of the polarization of the scattered light for some typical aerosol models with the aid of the Mie scattering theory.[1] The property of the scattered light intensity is also discussed with the experimental and theoretical results.

Experimental

The experimental system is schematically shown in Fig. 1. The N_2 laser with 25 Hz of repetition causes aerosol formation in the reaction cell (sphere glass with 25 cmϕ), which is filled with approx. fifty Torr† of carbon disulfide vapor. The polarized radiation of a He-Ne laser is introduced coaxially with the N_2 laser radiation, and the light scattered by the aerosol formed and the carbon disulfide vapor was measured in the direction perpendicular to the He-Ne

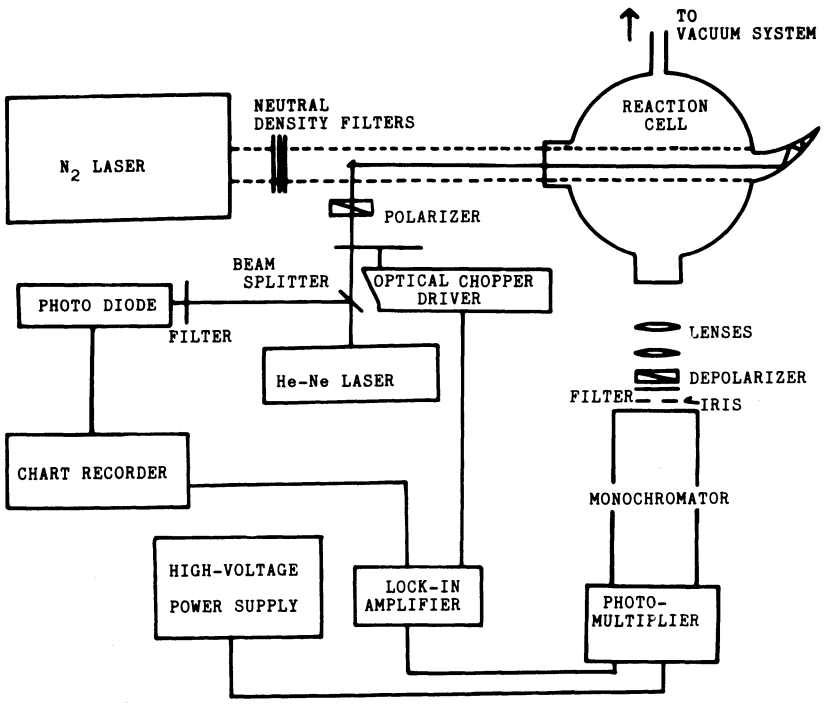

Fig. 1. Block diagram of experimental apparatus.

†1 Torr=133.322 Pa.

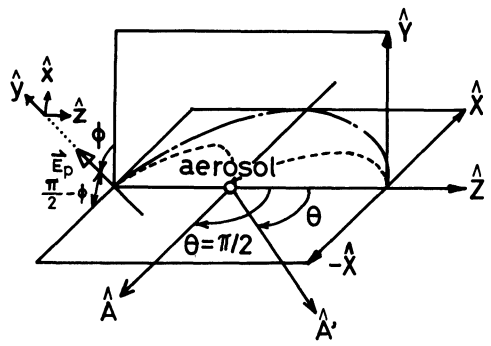

Fig. 2. Definition of the laboratory coordinate $(\hat{X},\hat{Y},\hat{Z})$ and the electric vector coordinate $(\hat{x},\hat{y},\hat{z})$. The angle between $\hat{Y}$ and $\hat{y}$ is ϕ. $\hat{A}$ and $\hat{A}'$ have the angles of $(\pi/2)$ and θ with the $\hat{Z}$-axis, respectively.

laser beam. Namely, lenses and an iris introduce the scattered light into a monochromator (f=200 mm) after the depolarization, then a photomultiplier detects it. The modulation of the He–Ne laser radiation with an optical chopper allows the measurement with a good signal-to-noise ratio by using a lock-in-amplifier detecting system. Carbon disulfide (Wako reagent grade) was used after the vacuum distillation.

Method of Theoretical Calculation

Definitions of Axes. For the convenience to describe these theoretical and experimental examinations, Figure 2 defines the laboratory-fixed axes $(\hat{X},\hat{Y},\hat{Z})$, the electric-vector-fixed axes $(\hat{x},\hat{y},\hat{z})$ and the angular parameters. The $\hat{Z}$-axis is coincident with the incident laser-beam axis. The directions of observation, *i.e.* $\hat{A}$ and $\hat{A}'$, are on the $\hat{X}$–$\hat{Z}$ plane and have the angles of $(\pi/2)$ and θ with the $\hat{Z}$-axis, respectively. The electric vector $\vec{E}_p$ of the incident laser beam is expressed in term of the $\vec{E}_p$ -fixed axes $(\hat{x},\hat{y},\hat{z})$. The $\hat{z}$-axis is in the same direction as the $\hat{Z}$-axis. The angle between the $\hat{y}$-axis and the $\hat{Y}$-axis is ϕ. For example, the Rayleigh-scattering angular distributions for the incident light polarized with ϕ=0° and 90° are shown by the dashed-solid line and the dashed line, respectively, in Fig. 2.

Outline of the Mie Scattering Theory. The exact solution to the scattering problem for a sphere radius r at wavelength λ was given by Mie in 1908,[1] elaborated by Debye,[2] and thereafter arranged by van de Hulst.[3] The problem is to obtain three dimensional solutions for Maxwell's equations for the electric and magnetic fields inside and outside a spherical region of radius r and the refractive index m at the frequency ω. By seperating the variables, solutions of the scalar wave equation $\nabla^2\psi+k^2m^2\psi=0$, where k is the wavenumber $(2\pi/\lambda)$, can be written in the spherical coordinates as:

$$\psi_{l,n} = \begin{matrix}\cos l\phi \\ \sin l\phi\end{matrix} P_n^l(\cos\theta)\left\{\sqrt{\frac{\pi}{2mkr}}Z_{n+1/2}(mkr)\right\}, \quad (1)$$

where Z represents either J- or H-solutions of Bessel's equation, P_n^l Legendre polynominals. A plane-incident scalar wave can be written:

$$u_0 = \exp(i\omega t)\cos\phi\sum_1^\infty(-)^n\frac{2n+1}{n(n+1)}P_n^1(\cos\theta)j_n(kr), \quad (2)$$

$$v_0 = \exp(i\omega t)\sin\phi\sum_1^\infty(-)^n\frac{2n+1}{n(n+1)}P_n^1(\cos\theta)j_n(kr). \quad (2')$$

The corresponding spherical Bessel functions are written by j_n and h_n. The scattered wave therefore contains only terms with l=1 and the scalar functions u and v can be written as:

$$u = \exp(i\omega t)\cos\phi\sum_{n=1}^\infty(-a_n)(-i)^n\frac{2n+1}{n(n+1)}P_n^1(\cos\theta)h_n(kr), \quad (3)$$

$$v = \exp(i\omega t)\sin\phi\sum_{n=1}^\infty(-b_n)(-i)^n\frac{2n+1}{n(n+1)}P_n^1(\cos\theta)h_n(kr). \quad (3')$$

The Mie solution process is one of finding a set of complex numbers a_n and b_n (Mie coefficients):

$$a_n = \frac{S_n'(y)S_n(x)-mS_n(y)S_n'(x)}{S_n'(y)[S_n(x)+iC_n(x)]-mS_n(y)[S_n'(x)+iC_n'(x)]}, \quad (4)$$

$$b_n = \frac{mS_n'(y)S_n(x)-S_n(y)S_n'(x)}{mS_n'(y)[S_n(x)+iC_n(x)]-S_n(y)[S_n'(x)+iC_n'(x)]}. \quad (4')$$

These complex-valued coefficients, functions of the refractive index m, $x=2\pi r/\lambda$ and $y=mx$ provide the full solution to the scattering problem. Here, S_n and C_n can be represented, as follows, with the Bessel functions $J_{n+1/2}(\rho)$ and the Neumann functions $N_{n+1/2}(\rho)$:

$$S_n(\rho) = \sqrt{\pi\rho/2}J_{n+1/2}(\rho), \quad (5)$$

$$C_n(\rho) = -\sqrt{\pi\rho/2}N_{n+1/2}(\rho). \quad (5')$$

The prime denotes differentiation with respect to the argument. The Mie coefficients give directly some important integrated quantities: The excitation, scattering and absorption efficiencies. The efficiency factors are defined as follows: The energy removed from an incident wave with energy flux density I_0 is $\pi r^2Q_eI_0$, Q_e being the extinction efficiency; the energy which reappears as scattered energy is $\pi r^2Q_sI_0$, Q_s being the scattering efficiency; the energy absorbed is $\pi r^2Q_aI_0$, Q_a being the absorption efficiency. These all can be written in terms of the Mie coefficients:

Extinction efficiency

$$Q_e = (2/x^2)\sum_1^\infty(2n+1)\mathrm{Re}(a_n+b_n), \quad (6)$$

Scattering efficiency

$$Q_s = (2/x^2)\sum_1^\infty(2n+1)\{|a_n|^2+|b_n|^2\}, \quad (7)$$

Absorption efficiency $Q_a = Q_e - Q_s$. (8)

Results and Discussion

The relationships between Q_s and the size of the aerosol particle are calculated for several refractive indices $1.5+im_{IM}$, m_{IM}=0, 0.01, 0.1, 1, 10, as shown in Fig. 3. Since x is the size parameter defined by $x=2\pi r/\lambda$ with an aerosol radius r and wavelength λ, x is proportional to r for a constant wavelength. Figures 4(a)—(f) show the angular distributions, *i.e.* θ-dependence, for x=0.01, 0.1, 1, 1.5, 2, 2.5 with m=1.55+0i. These figures indicate that, with the increase of x, (1) the forward scattering becomes predominant, (2) the perpendicular and parallel components of the scattered light intensities against the electric vector of the incident light, *i.e.* $I_\perp$ and $I_{/\!/}$, respectively, become greater and greater, (3) there is the intensity inversion between $I_\perp$ and $I_{/\!/}$ for the large x range, while $I_{/\!/}$ is always equal to or smaller than $I_\perp$ for $x\leq 1.5$, and (4) $I_\perp$ and $I_{/\!/}$ becomes oscillatory. The intensity inversion between $I_\perp$ and $I_{/\!/}$ causes the large variation of the polarization. The polarization is defined by $P=(I_\perp-I_{/\!/})/(I_\perp+I_{/\!/})$. Figure 5 shows the plot of P as a function of x. The polarization is nearly constant, *i.e.* approx. 1, for the range $x\leq 1.2$, then decreases steeply and gets to approx. −0.6 for

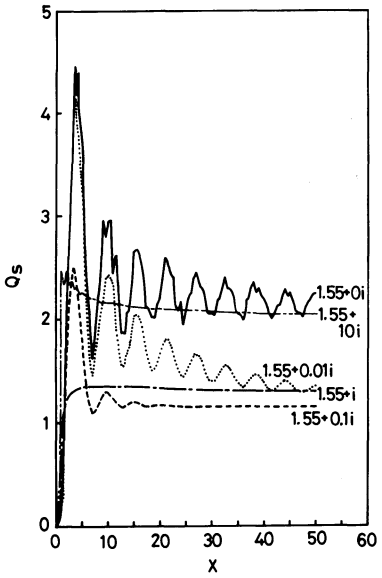

Fig. 3. The scattered light intensity Q_s versus the size-parameter x for $m=1.55+im_{IM}$, where m_{IM}=0, 0.01, 0.1, 1, 10.

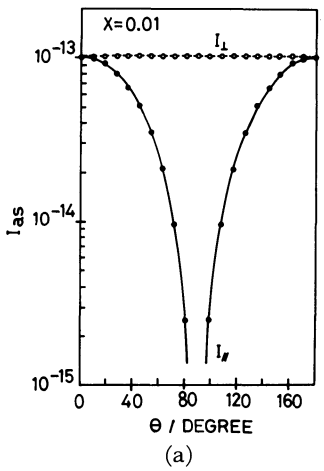

(a)

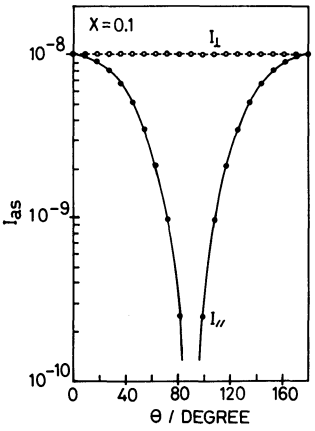

(b)

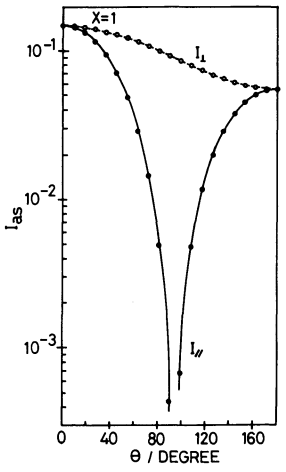

(c)

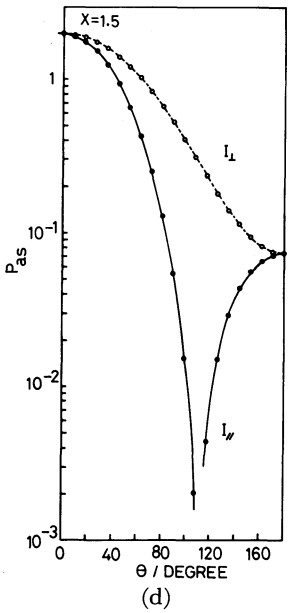

(d)

(Fig. 4. Continued on the next page)

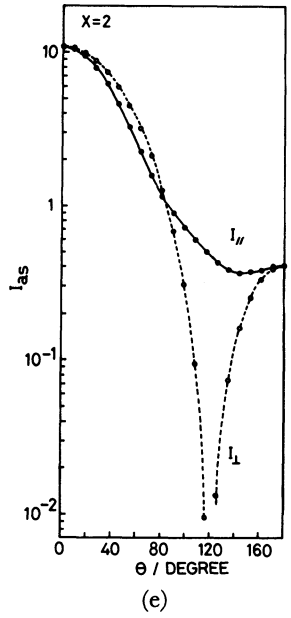

Fig. 4. The polarized scattered light intensities as a function of θ. $m=1.55+0i$.
(a) $x=0.01$, (b) $x=0.1$, (c) $x=1$, (d) $x=1.5$, (e) $x=2$, (f) $x=2.5$.

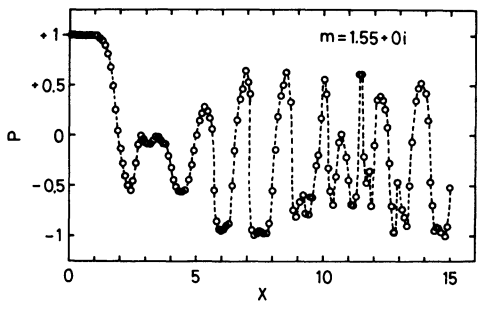

Fig. 5. Polarization P as a function of x, where $m=1.55+0i$.

$1.2 \leq x \leq 2.3$, and oscillates with the periods of $1 \leq x \leq 2$ and the amplitudes of $0.3 \leq P_{\text{peak-to-peak}} \leq 1.5$ for the range of $x \geq 2.3$. Therefore, as a function of the angle ($\phi - 90°$), the scattered light intensity in the direction of $\theta = 90°$

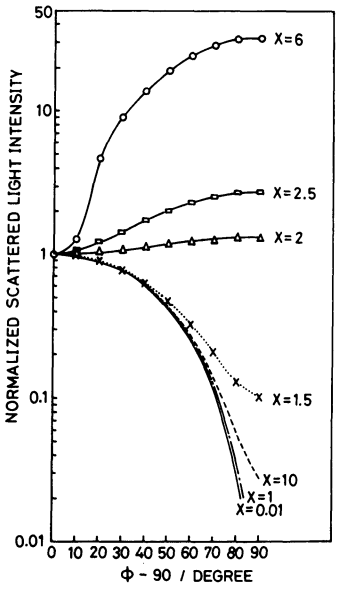

Fig. 6. The scattered light intensity calculated theoretically as a function of ($\phi - 90°$). $\theta = 90°$.

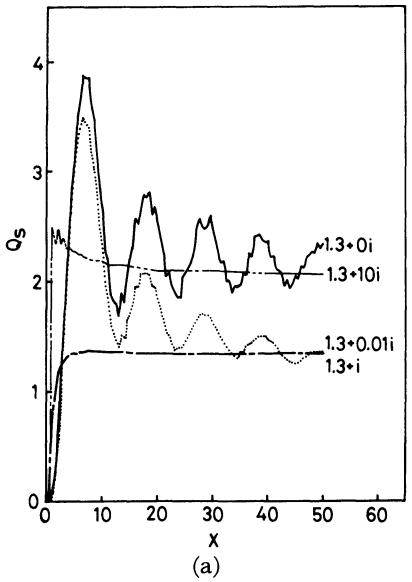

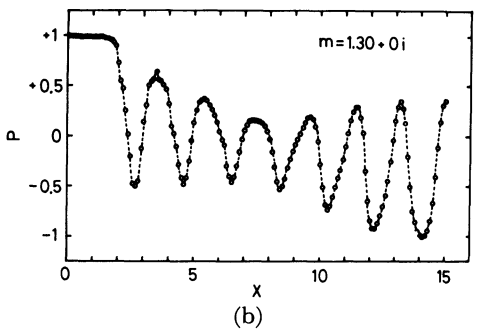

Fig. 7. (a) Scattered light intensity Q_s as a function of size parameter x for $m=1.3+im_{IM}$, where $m_{IM}=0$, 0.01, 1, 10, (b) Polarization P as a function of size parameter x, for $m=1.3+0i$.

can be theoretically estimated as shown in Fig. 6.

Furthermore, the scattering cross section Q_s and

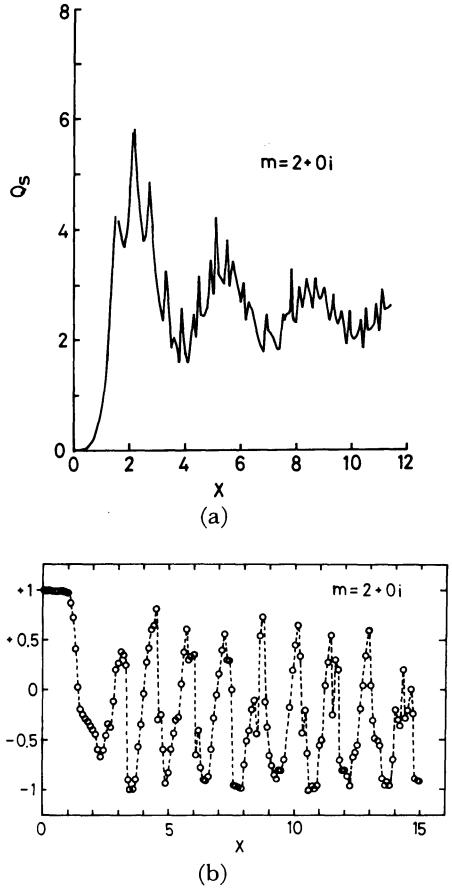

Fig. 8. (a) Scattered light intensity Q_s as a function of size parameter x, (b) Polarization P as a function of size parameter x, for $m=2.0+0i$.

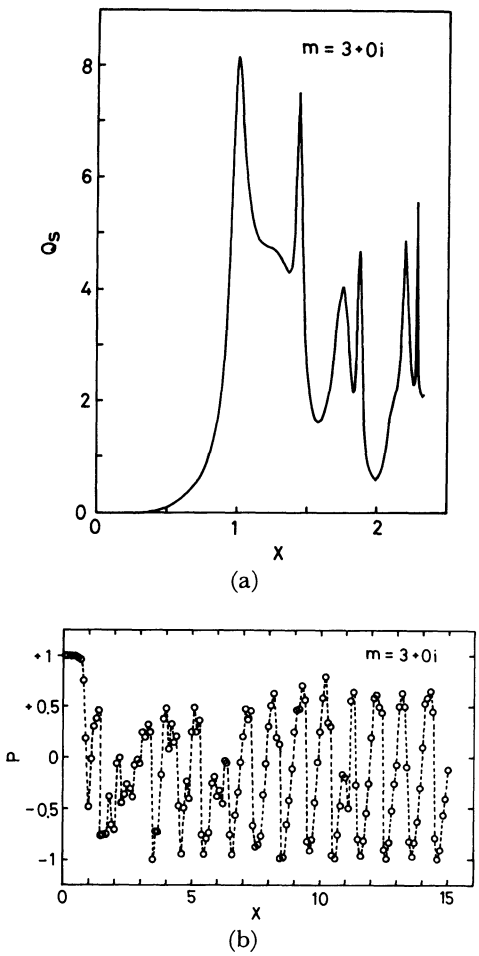

Fig. 9. (a) Scattered light intensity Q_s as a function of size parameter x, (b) Polarization P as a function of size parameter x, for $m=3.0+0i$.

the polarization P were also calculated for various indices, *i.e.* $m=1.3+im_{IM}$ ($m_{IM}=0$, 0.01, 1, and 10), $m=2+0i$, and $3+0i$, as shown in Figs. 7(a) and (b), 8(a) and (b), and 9(a) and (b), respectively. The essential shapes of the scattering extinction coefficients Q_s are similar for 1.3—2.0 of the real refractive index m_R, but Q_s becomes oscillatory with the increase in the real refractivity. The period becomes shorter. On the other hand, Q_s for $m_R=3$ has the different shape from those of $m_R=1.3$, 1.5, and 2. We can recognize the consistent characteristics of the polarizations for $m_R=1.3$, 1.5, 2, and 3. Namely, the steep decreasing of the polarization appears at smaller values of the size-parameter with the increase of the real refractive index. Furthermore, the polarization becomes oscillatory with the increase in the real refractive index.

The measurement of polarization has been used for experimental study on the size-growth in photoexcitation-induced aerosol formation.[4] However, the present study strongly suggests the caution for using this technique. Namely, since the polarization oscillates and becomes the same value for various size parameters, we cannot in general determine the size parameter from the polarization. In this view, the measurement of the angular distribution, *i.e.* θ-dependence, can be accounted much better for the study on the size-distribution of aerosol, as inferred from Figs. 4(a)—(f). Nevertheless, the polarization will be very useful for the judgement whether the scattering by the aerosol can be approximately expressed by the Rayleigh scattering[5] or not, *i.e.* the polarization is equal to 1 or not. As the application of it, this paper describes the experiments of the scattered-light polarization in laser-induced aerosol formation from gaseous CS_2.

In laser-induced aerosol formation, the light intensity scattered by the aerosol formed varies with time. The time evolution of the scattered light intensity in Fig. 10(a) is typical.[6] The scattered light intensity for the incident light polarized by the angle of $(90°-\phi)$ varies as a function of the angle $(90°-\phi)$, as shown by the open circles in Fig. 10(b). This ϕ-dependence was invariant for this time range. The dashed line in Fig. 10(b) is the curve of $\cos^2(90°-\phi)$, whose intensity is normalized to be 450 at $\phi=90°$. The experimental results agree well with the $\cos^2(90°-\phi)$ curve. By the comparison with the theoretical result shown in Fig. 6, the scattered light by the aerosol formed under the present experimental condition can be approximately expressed by the Rayleigh scattering theory. On the

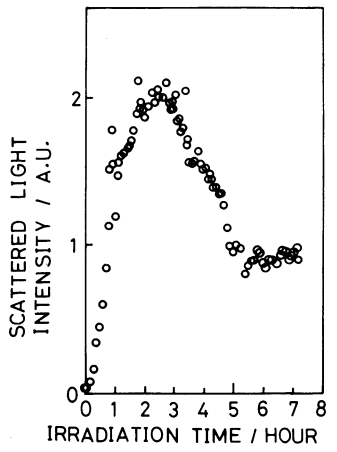

(a)

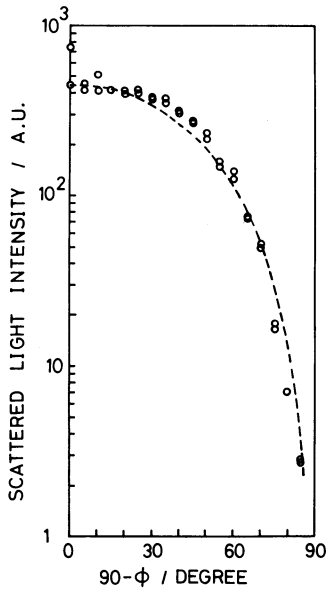

(b)

Fig. 10. (a) Scattered light intensity as a function of N_2-laser irradiation time. The CS_2 pressure is 50 Torr. The intensity of the N_2-laser beam was reduced by nuetral density filters. (b) Scattered light intensity as a function of $(90°-\phi)$. The dashed line is the curve of $\cos^2(90°-\phi)$.

other hand, the scattered light shows different behavior for the experiment with much more intense excitation N_2-laser beam, as shown in Fig. 11. In this case, the time-evolution of the scattered light intensity is quite different from that shown in Fig. 10(a). The polarization is less than 1 and varies with time. Therefore, in Fig. 11, the radius of the aerosol particle is large and the scattered light behavior cannot be expressed by the Rayleigh scattering theory.

The scattered light intensity has been extensively used as a kind of concentration variable. Since the scattered light intensity can be expressed by $\pi I_0 \int_{-\infty}^{+\infty} r^2 Q_s N(r) dr$, it depends upon the radius and concentration of aerosol. If the aerosol is small enough, the scattering intensity behavior is in the Rayleigh scattering range, *i.e.* it can be expressed as:

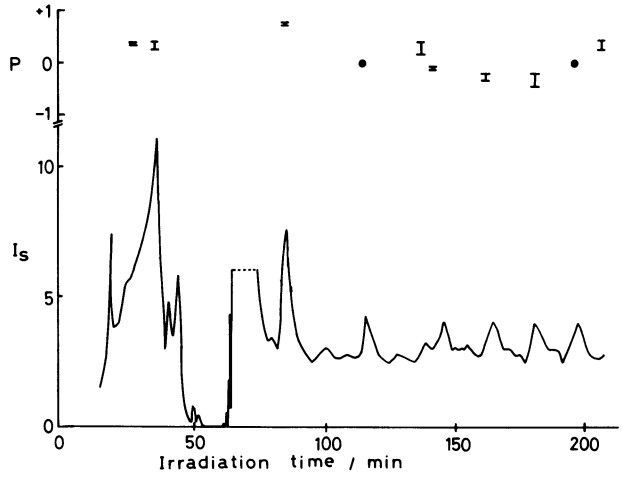

Fig. 11. The polarization P and scattered light intensity I_s as a function of N_2-laser irradiation time.

$$I = \frac{\omega^4}{c^4 R^2} \alpha^2 (1+\cos^2\theta) N(r) I_0, \tag{9}$$

$$I = \frac{\omega^4 r^6}{c^4 R^2} \left(\frac{m^2-1}{m^2+2}\right)^2 (1+\cos^2\theta) N(r) I_0, \tag{9'}$$

where R is the distance from the aerosol, ω the frequency of the scattered light, and c the light velocity. The polarizability α can be expressed by

$$\alpha = \frac{3}{4\pi N_s}\left(\frac{m^2-1}{m^2+2}\right), \tag{10}$$

where N_s is the total number of molecules per volume, and m is the nondimensional refractive index of molecules. Equation 9′ suggests that the scattered light intensity is proportional to the number of aerosol, $N(r)$, and the sixth power of the aerosol radius. Therefore, for the Rayleigh scattering range, the scattered light intensity can be expressed by $I=c_1 r^6 N(r)=c_2 v^2 N(r)$, where c_1 and c_2 are constants, $N(r)$ the number density, v the volume of aerosol, as a kind of extensive variable. Since the total number of molecules in the aerosol, N_m, can be considered proportional to the volume v, the scattered light intensity can also be expressed by $I=c_3 N_m^2 N(r)$, where c_3 is a constant. Thus the *trajectory tracing approach*[6] is applicable by using the scattered light intensity for the Rayleigh scattering range. On the other hand, more complicated process will be required for the case shown in Fig. 11. Nevertheless, since the maximum entropy method used in the *trajectory tracing approach*[6] is a kind of nonlinear spectrum analysis, it can make the analysis of the oscillatory behavior of the scattered light intensity for the size-parameter range, where Q_s increases with the size-parameter, even if it is out of the Rayleigh scattering range.

References

1) G. Mie, *Ann. Phys.*, **25**, 377 (1908).

2) P. Debye, *Ann. Phys.*, **30**, 59 (1909).
3) H. C. van de Hulst, "Light Scattering by Small Particles," Wiley, New York, (1957), p. 470.
4) T. Sato, T. Yabuzaki, and T. Ogawa, *J. Appl. Phys.*, **21**, 1599 (1982).
5) L. Rayleigh, *Proc. Lond. Math. Soc.*, **10**, 4 (1879).
6) A. Matsuzaki, *Chem. Lett.*, **1983**, 1149.